Additive Manufacturing 33 (2020) 101146

Contents lists available at ScienceDirect

Additive Manufacturing

journal homepage: www.elsevier.com/locate/addma

Full Length Article

An automated system for 3D printing functionally graded concrete-based materials

Flávio Craveiro[a,b], Shadi Nazarian[c], Helena Bartolo[a,b], Paulo Jorge Bartolo[d], José Pinto Duarte[c,*]

[a] CIAUD, Lisbon School of Architecture, Universidade de Lisboa, Portugal
[b] School of Technology and Management, Polytechnic Institute of Leiria, Portugal
[c] SCDC, School of Architecture and Landscape Architecture, The Pennsylvania State University, USA
[d] School of Mechanical, Aerospace and Civil Engineering, The University of Manchester, UK

ARTICLE INFO

Keywords:
3D printing
Additive manufacturing
Building automation
Digital fabrication
Functionally graded materials
Concrete printing

ABSTRACT

In recent years, the interest in developing additive manufacturing (AM) technologies in the architecture, engineering and construction (AEC) industry has increased, motivated by the potential to support greater formal complexity. In this context, AM has been largely used to design and fabricate physical parts with homogeneous materials. This paper proposes a new strategy, aimed at the design and fabrication of functionally graded concrete parts with specific thermo-mechanical performance. The paper describes the development of the AM system to materialize such parts. The computational tool developed to design the material to meet specific performance requirements, and the design and testing of the material are described elsewhere. A functionally graded concrete part obtained by replacing sand with cork was produced and is evaluated.

1. Introduction

Digital transformation and innovation are major driving challenges for the architecture, engineering and construction (AEC) industry, creating a unique opportunity for a disruptive change in the construction ecosystem, and a huge opportunity towards a whole new way of working and integrating services (consulting, design and fabrication). Digitally based construction methods have the potential to boost construction productivity and efficiency, allowing greater design freedom and work safety. According to Shomberg [1], the combined use of robotics and 3D printing permits to use 30%–60% less material, reduce waste and build 50%–80% faster.

3D printing technologies, also called additive manufacturing AM technologies, refer to a class of manufacturing processes in which a part is built by adding layers of material upon one another. These technologies became popular in the 1990s with the fast production of conceptual product models, mainly for aesthetic and ergonomic purposes. Today, there is a wide range of AM technologies applied in a variety of industries, including the aerospace, automotive, and medical industries, as well as in the AEC industry. According to ISO/ASTM 52900:2015 standard [2], AM technologies currently available are material extrusion, material jetting, binder jetting, sheet lamination, vat photopolymerization, powder bed fusion and direct energy deposition. However, in the construction sector, the most used processes are binder jetting and extrusion-based processes.

Extrusion processes are based on print-heads (nozzles) [2] mounted on frames, robots or cranes [3,4] that deposit successive layers of building material, frequently concrete, from the base to the top of the structure. Today, large structures are already being manufactured using concrete extrusion technologies [3–6], such as an office in Dubai produced by Winsun [7] or the house built by Apis Cor [8], as well as, a full-scale bridge made by TU Eindhoven [9], vertically printed components by Loughborough University [10], and 3D printed multifunctional walls geometrically optimized according to thermal or acoustical criteria by Gosselin et al. [11].

These technologies are commonly used to fabricate structures with homogeneous materials [12,13], designed to resist to maximum stress. Quite often, the use of material resources is higher than required [14–16] in traditional construction processes, as full strength might be required only in specific areas [17,18]. On the other hand, the use of functionally graded materials (FGM), inspired by nature [19–21], characterized by a spatial change in material properties regarding composition and microstructural gradient, can be customized to specific thermo-mechanical loading conditions. Both the composition and the structure can gradually change over the form, resulting in varying material properties. The direction of the gradient can determine its features and performance, resulting in lightweight structures with enhanced mechanical properties with an optimized distribution of mass

* Corresponding author.
E-mail address: jxp400@psu.edu (J. Pinto Duarte).

https://doi.org/10.1016/j.addma.2020.101146
Received 21 September 2019; Received in revised form 13 January 2020; Accepted 20 February 2020
Available online 22 February 2020

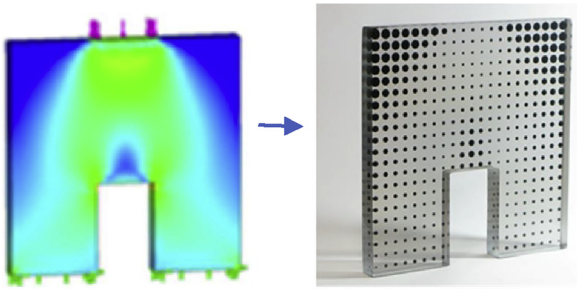

Fig. 1. Single-material composition: porosity optimization according to internal stress [22].

and improved thermal insulation capabilities. Gradient structures with optimized mass distribution can be achieved through single-material or multi-material compositions.

In single-material compositions (geometry-based gradient structures), the same material contains more holes in specific locations, creating lighter regions, with denser locations presenting higher strength. Fig. 1 presents previous work [22] aiming at improving the material composition of a concept wall prototype subjected to a vertical load. The material was designed through an algorithm, which permits to generate variable density by changing the number and size of internal pores, according to stress concentration results, previously obtained by finite element analysis (FEA). To allow a better visualization of the porosity spatial distribution and size, the concept wall prototype, was materialized by AM technologies (Polyjet Connex 3) using transparent and opaque materials, with opaque material representing holes.

Several research groups have been investigating the production of mass-optimized concrete components containing a tailored distribution of pores, also produced by AM technologies [17,23,24]. MIT Mediated Matter group [23] developed a strategy to extrude concrete with varying density by gradually mixing concrete with aluminum powder and lime, which react to produce hydrogen gas bubbles responsible for creating a foaming structure. Conversely, Chee et al. [24] used a robot together with a controlled syringe dispenser to inject an aluminum solution in specific locations of a white cement panel, creating personalized patterns of holes [24].

In multi-material compositions, manufactured components present gradient transitions between two or more different materials, either containing porosity gradation or not. A smooth transition between materials helps to minimize residual stresses caused by the heterogeneity of materials, reducing common failures, such as cracks and delamination [25,26].

Cementitious materials, particularly concrete, are the most widely used construction materials in the world, either for traditional or layered construction [6,11,27]. Moreover, there is an increasing pressure to use recycled aggregates processed from industrial waste materials, as a solution to reduce the depletion of earth natural resources [28–32]. A good example is the cork industry, where only 25 % of the harvested cork is used to produce high quality punched bottle stoppers, with the remaining 75 % rejected and then granulated and used for other diverse industrial applications. In the construction sector, this granulated cork is mainly used for thermal and acoustic insulation, or as a lightweight aggregate for concrete and mortars [33–35].

Lightweight aggregates can be used to produce functionally graded concretes with multifunctional properties, minimizing its total mass and increasing thermal properties [26,36,37]. This idea was explored by Herrmann and Sobek [17] which manufactured structural components with optimized mass and thermal performance by gradually adding lightweight aggregates to a higher-strength fine-aggregate concrete, using graded spraying techniques [17].

On the other hand, our group has been developing extrusion-based systems to 3D print homogeneous concrete parts, as well, functionally graded polymer ones [36,38]. Consequently, it was decided to extend

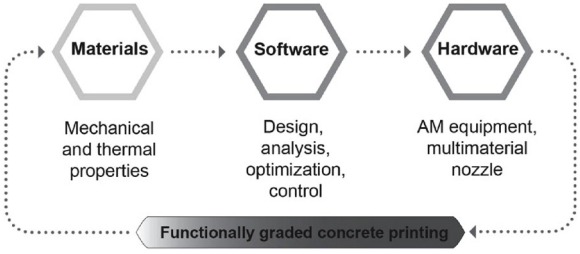

Fig. 2. Components of the functionally graded concrete printing system.

the development of extrusion techniques to produce functionally graded concretes using cork as a lightweight aggregate, which requires the development of software, hardware and materials, with the desired behavior, as illustrated in Fig. 2.

Craveiro et al. [26,39,37] details the software and demonstrates that an adjusted distribution of the material composition according to the internal principal stress can minimize the total weight of the structure by using lightweight aggregates in areas with less strength requirements. In addition, the thermal properties of these aggregates help improve the global thermal performance of the walls, reducing the energy consumption needed to keep the interior temperature at certain level, when compared to non-functionally graded walls.

The development of printable materials containing cork [40–42] shows that thermal properties improve with the addition of cork, while mechanical properties decrease.

This work is focused on the hardware part of the system and it presents additive manufacturing technology capable of fabricating functionally graded building parts according to multiple performance requirements, using functionally graded concrete as the building material. The paper details the developed hardware and presents different produced parts, namely homogeneous and functionally graded concrete parts, which are then evaluated to verify the ability of the system to produced parts with the desired properties.

2. A new AM system: software and hardware

A novel AM system, comprising both software and hardware was developed to produce single material and multi-material functionally graded structures.

2.1. Software

The software, developed in Grasshopper/Rhino 5.0, allows the design and fabrication of functionally graded building components according to structural and thermal specifications, combining parametric design, structural and thermal analyses, as well as a materials database to design improved heterogeneous materials [37]. The code is clustered in three modules, presenting a user-friendly interface in Grasshopper, as shown in Fig. 3. The toolpath & robot simulation module supports the design of straight or curved building walls, with or without openings, as well as specifying the position of applied loads and supports for simulation purposes. It also permits to import toolpaths and control the movements of the robot. The material design module allows to discretize the building elements into voxels and import mechanical and thermal analysis results by image diagrams sampling or by using. CSV files with FEA x-y-z node coordinates. The mapping between voxels and the corresponding FEA nodes is critical to assign material properties. Material definition is performed using a material database where materials are characterized by empirical models, correlating composition and mechanical and thermal properties [37,39]. Each material composition is related to a specific pump speed ratio.

This parametric tool controls the pump speed and the print head spatial displacement, according to predefined material and shape designs. Another module utilizes data from the previous modules and uses

a)

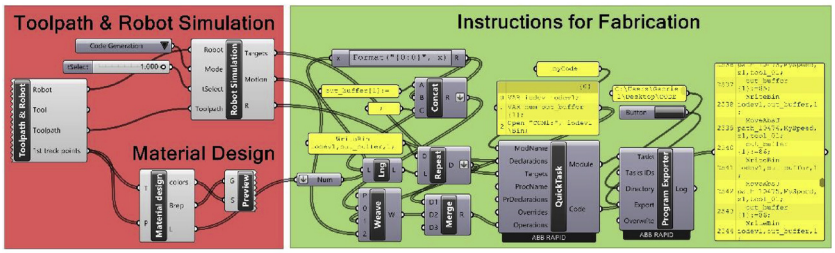

b)

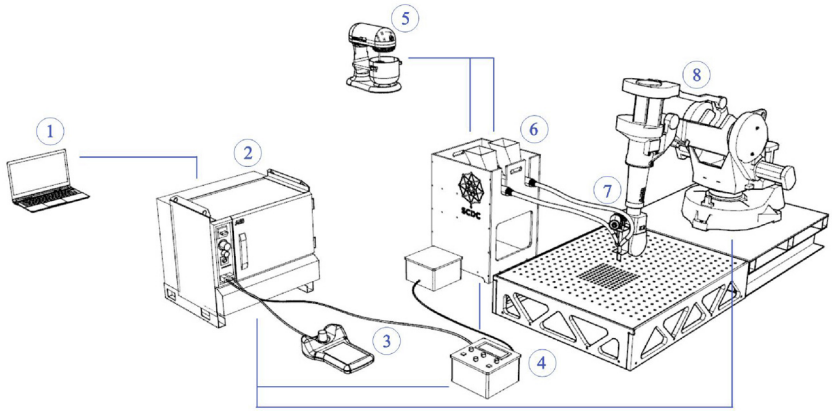

Fig. 3. AM system: a) Generative tool (1. grasshopper code, 2. visual output in Rhinoceros showing the varied material composition, translated in a graded color); b) Diagram of the AM of concrete system (1. Computer for designing the material and the toolpath and generating the robot code, 2. Robot controller model IRC 5, 3. Robot tech pendant for hand control, 4. Pumps tech pendant for hand control, 5. Mixer for materials preparation, 6. Concrete pumps, 7. Dynamic mixer/ extruder nozzle, 8. Robotic arm ABB IRB 2400).

the HAL robotics plug-in to generate a. RAPID file, that contains the instructions for controlling both the robotic arm and the pumps. It also outputs a visual simulation of the process to Rhinoceros showing the robotic arm displacements and the fabrication process. A color gradation matching material composition allows one to gain a better understanding of the target result as shown further below.

2.2. Hardware

2.2.1. Robot

The hardware (Fig. 5.2b) consists of a 6-axis robotic arm (ABB IRB 2400) used to guide a novel printing head [43]. This robot reaches a maximum of 1.55 m with a handling capacity of 16 kg, and so the deposition system was developed considering the following constraints:

- The pumps and other heavy components should stand near the building area;
- The weight of the printing head and the building materials flowing from the pumps should remain under 16 kg;
- The print head should be attached to the gripper tool flange of the robotic arm;
- The working range is 1000 × 800 × 1500 mm;
- The pumping system should be capable of extruding fine-aggregate concrete;
- The hardware must be fully automated and yet have the capacity to be fine-tuned in real-time by the user.

2.2.2. Pumps & flow rate control

A feeding system based on two pumps (Quickpoint mortar pumps) allows supplying the materials to the printing head, from two individual reservoirs where single materials are kept at room temperature. Each pump (Fig. 4a) comprises (1) a concrete container that receives homogeneous material previously prepared in the mixer, (2) a delivery pipe coupling, (3) unblocking blades to avoid clogs inside the chamber, (4) an extruder screw to compress and push the material through the tube, (5) a barrel that receives the extruder screw, (6) a vibrating rod to help the material flow to the barrel, (7) a cam coupling to connect the motor, and (8) a motor (Dewalt DW130) to rotate the extruder screw. Both pumps stand near the robot and feed the extrusion heads through ¾" flexible pipes 800 mm long. Each pump reservoir holds a single material, previously prepared in the mixer (Fig. 3b). Each pump reaches a maximum flowrate of 6.2 cm^3/s.

By gradually changing the volume fraction of each constituent material, which can be accomplished by changing the relative speed of pumps, it is possible to manufacture functionally graded structures. Smooth transitions lengthwise the extruded filaments allow to create continuous graded compositions, while stepwise gradients are produced along different filaments, creating small discontinuities in the material composition (Fig. 4b). Reducing the diameter of the filaments will decrease the discontinuities but increase the printing time.

To synchronize the pumping flow rate according to the spatial displacement of the printing head, an Arduino-based interface composed by two control modules, connected to the robotic arm controller, was also developed. The material composition gradient can be adjusted by continuously changing the pumps' speed ratio. The pumps' control modules ensure that the extrusion process is synchronized with the robot movements, by receiving digital DC signals from the serial port of the robot controller (IRC5), and continuously adjusting the speed of each pump (Fig. 5).

The robot code is compiled in RAPID (ABB language), which includes a function called *WriteBin*, used to send a binary signal through the serial port of the IRC5 controller. As the printing process requires not only determining the spatial position of the printing head but also potentially changing the material composition during consecutive positions of the robot arm, it was necessary to consider multiple intermediate positions between two main points, allowing incremental adjustment of the material composition. At each new location, an updated binary number is sent from the robot and then read by the control modules, which update the pumps speed ratio. This way, the required combination of materials is created at the desired location. Better material definition can be obtained by increasing the number of intermediate points. The control modules are composed by two Arduino based micro-controllers, as illustrated in Fig. 5.

Control Module 1 is composed of an Arduino Mega 2560, a RS-232

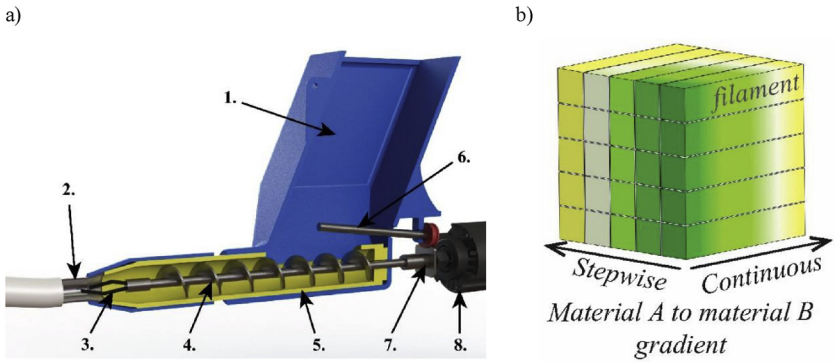

Fig. 4. a) Fine aggregate concrete pump detail; b) material gradient according to the direction.

shield, analog buttons, and an LCD screen. This module is connected to the robot controller by a serial cable to continuously receive binary numbers ranging from 0 to 99. Zero corresponds to 100 % speed for pump 1 and 0% speed for pump 2, while 99 corresponds to speeds of 0% for pump 1 and 100 % for pump 2, respectively. The ratio of each pump can also be tuned by the user, using the analog potentiometers. The LCD screen presents the value received from the robot and the corresponding pump ratio, which is sent by I2C protocol to Control Module 2.

Control Module 2 is composed of an Arduino and two power control modules. The Arduino is programmed to receive the ratio of each pump by I2C protocol, and to control both pumps rotational speed through the power control modules. These modules are composed of three main components: an optocoupler, a triac (BT139-600E) and a snubber circuit. The 110 V alternating current (AC) power delivered to each motor is controlled by defining the time within which the triac will be conductive, counting from the zero point of the input AC waveform, allowing only a part of the waveform to be delivered to the motor. The zero cross occurs twice during a full wavelength (period of 360°), so θ can take values from 0° (full power) to 180° (no power). A zero cross detection circuit analyses the input power and detects when the waveform crosses the 0 point, sending this information to the Arduino. The optocouplers use light to transfer electrical signals between the two isolated circuits, namely the 110 V AC motor circuit and the 5 V DC Arduino circuit, protecting Modules 1 and 2, as well as the robot from high voltages.

2.2.3. Print heads

Several designs were attempted for the multi-material printhead. First, a simple printhead was used (Fig. 6a) and then tested by adding a colorant to the material in one of the pumps, to verify if the printhead was effective in mixing the materials from the two pumps into a single continuous filament. As observed (Fig. 6b), the materials were not properly mixed, leading to the design of a printhead with a dynamic mixer (Fig. 7) to guarantee good mix and flowability of the material, as can be observed in Fig. 14.

This new printhead is formed by a metal body with two material inlets and one nozzle with 15 mm of internal diameter. Internally, a

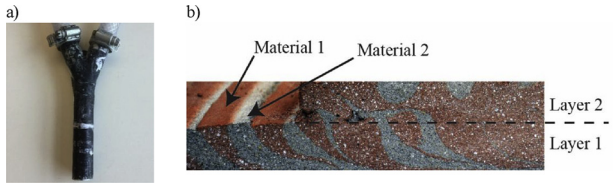

Fig. 6. a) Y shape nozzle, and b) cross-section of a printed 2 material specimen printed with the Y shape nozzle.

stainless-steel mixing rod is composed of 8 mixing blades, disposed with an angle of 15° relative to the flow. The spin is assured by a 12 V DC high torque motor Valeo 579053. The mixing chamber is 80 mm long, which is the path length required to produce a new gradation, after a sequent change of pump speed ratio. The speed of the mixing rod was defined by the flow simulation study described in Craveiro et al. [43].

3. Case studies

3.1. Geometrical and material design

A curved external wall with a customized material composition was chosen as a case study. Two material conditions were considered for this element of the building envelope:

- Case study 1: Single material;
- Case study 2: Functionally graded material.

In the first case, a homogeneous fine aggregate fiber-reinforced Portland cement concrete was used to calibrate both software and hardware of the 3D printing system (i.e. set maximum robot and pump speed according to the material and assess the toolpath design). In the second case, two different materials were used to create a functionally graded curved external wall, by changing the ratio between them. In this case, the curved external wall was designed to provide good insulation properties to the outdoor side of the wall, using a material with low thermal conductivity to create an efficient heat barrier, which is gradually replaced by a material with higher thermal inertia to offer

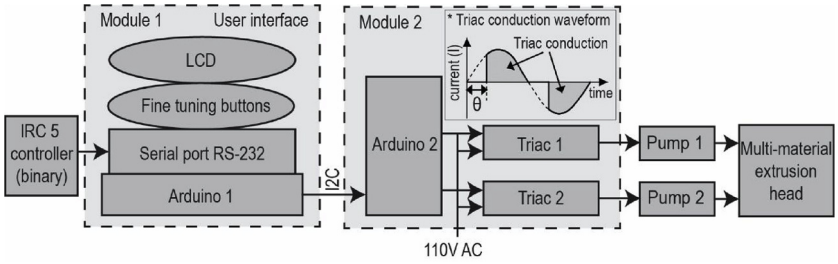

Fig. 5. Multi-material extrusion system diagram presenting the control modules.

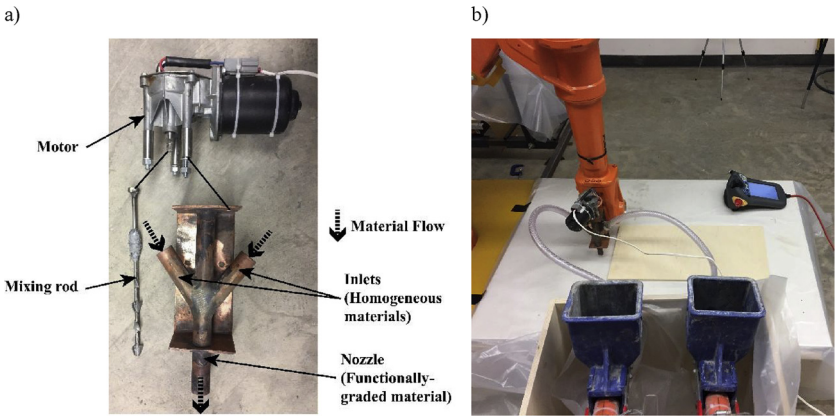

Fig. 7. Dynamic printhead: a) detail view, and b) coupled to the robot and pumps.

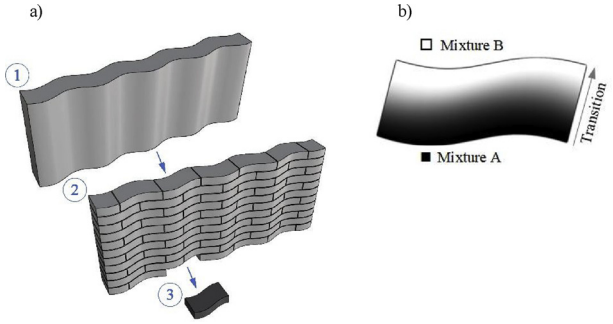

Fig. 8. Case study: a) visual output in Rhinoceros showing the computed curved wall including the initial shape (1), the wall subdivided into discrete blocks (2), and one block unit extracted (3); b) scheme of the gradient transition from Material A to Material B (top view).

Table 1
Material properties [41].

Material	Density	Thermal conductivity	Compression strength
M0cork	1.98 kg/dm^3	0.82 W/(m × K)	42.22 MPa
M10cork	1.86 kg/dm^3	0.73 W/(m × K)	34.36 MPa

improved indoor comfort. An algorithm was developed to create subdivisions with non-uniform properties regarding shape and material composition, splitting the wall into small block units (Fig. 8a). One heterogeneous block unit was produced using the abovementioned equipment. Each block unit can be produced with a spatially varying composition, gradually changing from "Material A" to "Material B" (Fig. 8b). To ensure an optimal material cohesion and compatibility along the seamless transition, a fine aggregate fiber-reinforced Portland cement concrete was used as the main binder in both Materials A and B, and is composed of 11.78 wt% of water, 23.58 wt% of cement, 51.52 wt % of basalt sand, 0.07 wt% of basalt fibers (1/4 "), 1.81 wt% of silica fume, 10.88 wt% of slag, 0.25 wt% of superplasticizer and 0.02 wt% of a lime replacement admixture [41]. In the case of Material B (M0cork), basalt sand was used as single aggregate, while in Material A (M10cork) 10_{vol}% of the basalt was replaced by granulated cork, which is a natural lightweight material with remarkable thermal properties. Table 1 shows, for both mixtures, the hardened material density, thermal conductivity and compression strength.

These properties vary linearly according to the percentage of cork replacing sand. Detailed material composition, mechanical and thermal properties are presented in Craveiro et al. [40] and Craveiro et al. [41]. Replacing sand by cork in specific areas also contributes to reducing the weight of the wall, ensuring its structural integrity [37].

The printing tool paths were computed and generated considering several constrains, such as the robot's work envelope, the pumps output capacity, the nozzle size, and material rheological properties (Fig. 9).

3.2. Printing process

3.2.1. Homogeneous material

Four homogeneous components were produced using two different toolpaths (contour and zigzag), as shown in Fig. 10. First, three standard elements (Fig. 10a) were produced. These elements were designed and materialized with a specific material (metakaolin geopolymer) for a NASA challenge, namely a truncated cone for a shape accuracy test, a cylinder for ASTM C39 compression test and a beam for ASTM C78 flexure test. This composite material was used for this challenge because of the availability of its component materials on the Mars regolith. The printing of these materials helped fine-tune the process before printing functionally graded materials. The truncated cone (base diameter 200 mm, top diameter 100 mm, and height 300 mm and the cylinder (diameter 150 mm and height 300 mm) were both printed at the speed of 35 mm/s considering twenty-three horizontal layers. The beam (length 650 mm, width 100 mm, and height 200 mm, and 100 mm) was extruded at a speed of 25 mm/s. All the components were built within a tolerance of +/−7 mm [42]. Different tool paths were also tested (Fig. 10b), as its design can influence print quality. For instance, tight curves and direction changes can create significant underfill in zones supposed to be completely dense. Second, a single curved block unit with the shape presented in Figs. 8a and 9 a and b was printed and evaluated (see subsection 3.2.1.1).

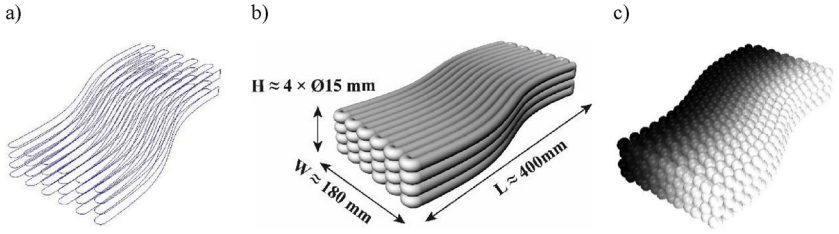

Fig. 9. Curved block unit: a) tool path, b) CAD model showing the dimensions and the layering of filament (4 layers), c) CAD model presenting the material gradient.

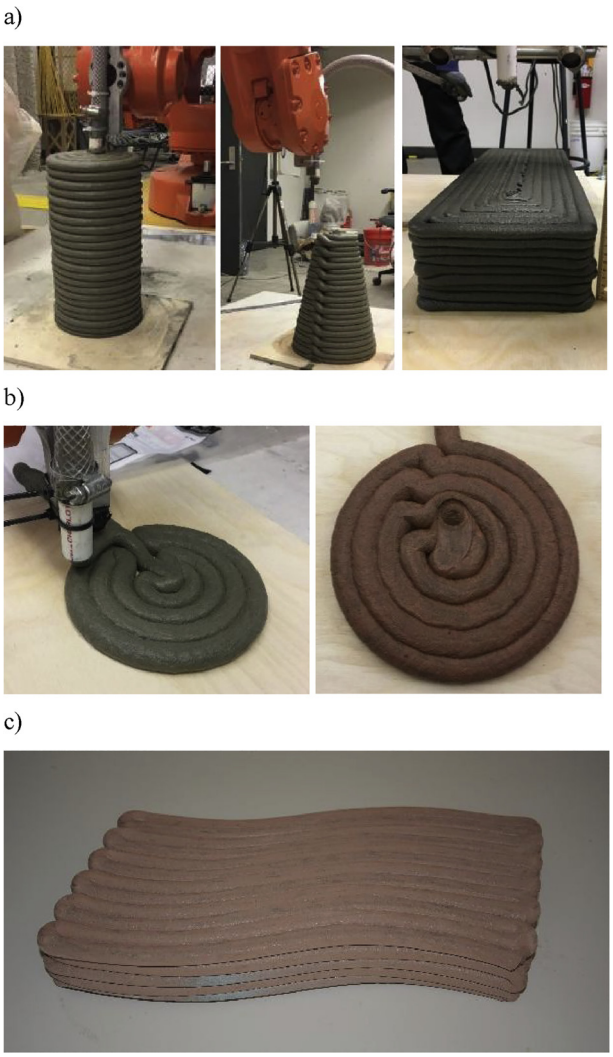

Fig. 10. Homogeneous structures produced by AM: a) curved block unit, b) cylinder, cone and beam produced [42], c) different tool paths of a cylinder (first layer) (One of the parts was produced with the colorant later used to verify the mixing capabilities of the dual material system).

3.2.1.1. Case study 1. The single curved block unit presented in Fig. 10c was printed at a deposition speed of 25 mm/s using M0cork material. A preliminary geometrical evaluation of the homogeneous curved block unit was conducted, after the curing period, using a 3D Systems Sense 3D scanner (resolution ~1 mm). The point cloud was saved in a. OBJ file and the geometry was cleaned with Geomagic Studio 12. Then, Geomagic Qualify 12 was used to compare the 3D scanned geometry and the predicted design (Fig. 11). The results present a standard deviation of 4.163 mm. Some deviation peaks can be observed on the vertical curved side walls (orange color), where the outer filaments tend to slide out, due to bigger sinking (blue color), possibly caused by toolpath design or material deformation after deposition. To get a better understanding of the origin of deformation, the block was sectioned into half using a diamond electric saw. Fig. 12 presents the component's cross section, allowing for internal visual assessment. On the right side of the section, it can be observed the detachment of external filaments and the presence of voids, corresponding to the zone of higher formal deviation. Voids between filaments are also present in the upper layer, possibly due to the lack of pump pressure and-or to the excessive distance of the nozzle to the previously printed layer, as there was no compensation for material deformation due to the deposition of subsequent layers.

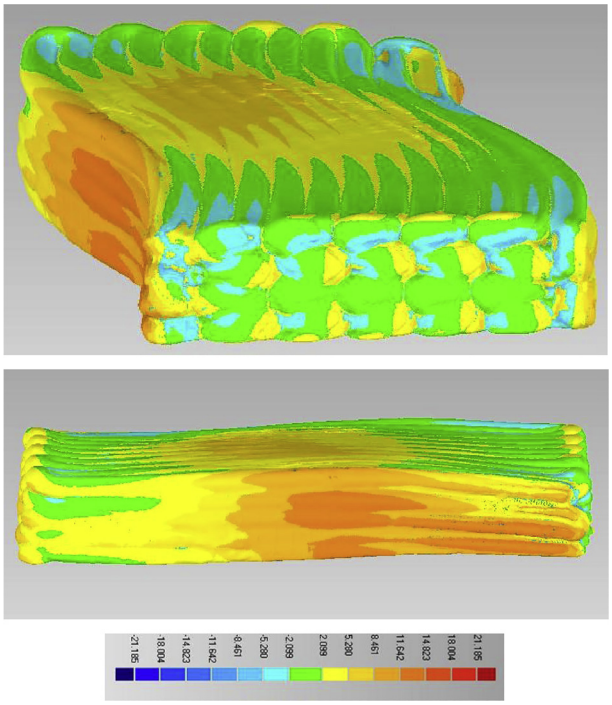

Fig. 11. Deviation analysis of the homogeneous curved block unit.

Fig. 12. Cross section of the homogeneous curved block unit.

3.2.2. Case study 2

A functionally graded single wall block unit (Fig. 9) made by a gradation of two different fine-grained concretes was produced. In this case, each pump reservoir holds a single material, one containing a sand-based concrete mixture (M0cork) and the other a mixture in which cork granules replace 10_{vol}% of sand (M10cork) (Fig. 13a).

Based on both material composition and printing instructions, the materials were extruded through the dynamic nozzle. The thickness of each filament was 15 mm, and the printing speed 25 mm/s. These values were selected after several tests, conducted through an iterative process, considering material flowability and hardware limitations (e.g. pump pressure).

After 7 days curing, the printed block was sectioned in 3 parts (Fig. 13c) to verify the distribution of cork. Fig. 13d shows the middle cross-section (Section 2) of the printed block. It is possible to observe a gradation of cork replacing sand, varying from 0 % (left) to 10_{vol}% (right). Some voids are observed due to insufficient pressure of the pumps.

ImageJ, a Java-based image processing software created at the National Institutes of Health [44], was utilized to evaluate the distribution of cork granules along the three cross-sections (Fig. 13c). Each cross-section image was prepared and imported to the software, wherewith a granule of cork was selected and used as target. The software analyses the image and highlights similar areas, converting it into red spots. Due to the presence of voids in the cork zone (right), a delimited area, shown in Fig. 13d, was then evaluated. The same

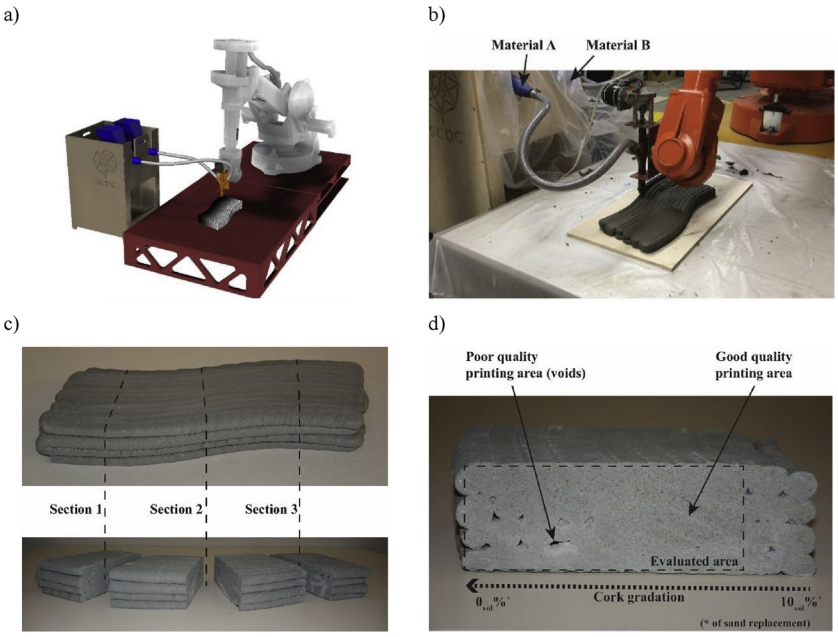

Fig. 13. a) Simulation of the printing process, b) 3D printing process, c) printed element and sectioned areas, d) cross section detail (Section 2) of the printed component.

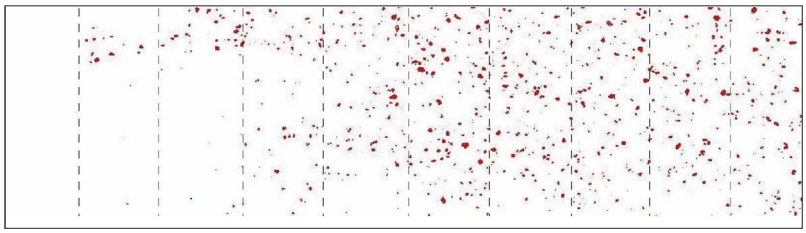

Fig. 14. Middle cross-section evaluated in ImageJ highlighting the cork particles and presenting the location of the filaments.

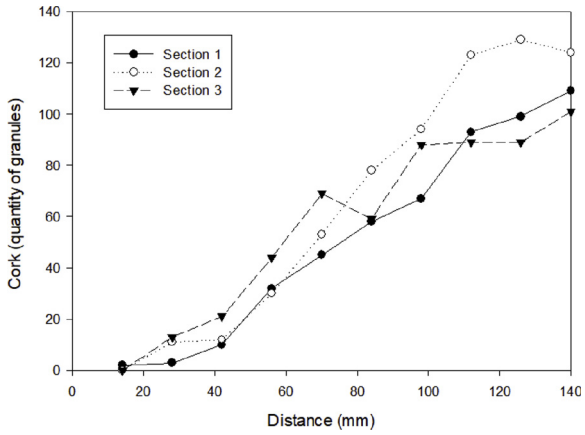

Fig. 15. Cork distribution in the 3 cross-sections.

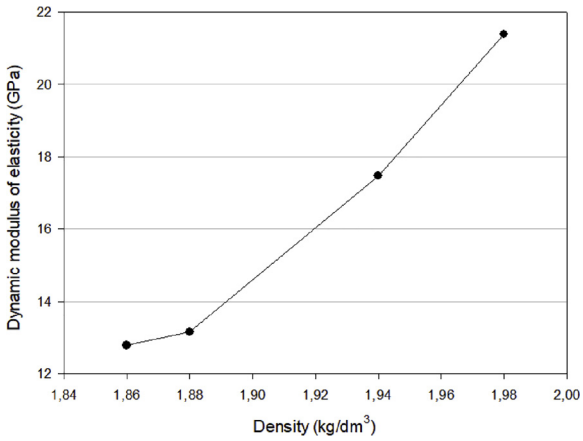

Fig. 16. Dynamic modulus of elasticity vs density.

criterion was applied in all the cross-sections. Highlighted cork distribution along the middle cross-section (Section 2) is shown in Fig. 14. Each evaluated area was then divided in 10 zones along the gradation direction and ImageJ was used to count the number of visible cork granules in each one. The distribution of cork content is presented in Fig. 15. A gradual increase in quantity can be perceived in all the 3 cross-sections.

Additionally, to determine the dynamic modulus of elasticity (E) by Impulse Excitation Technique, four rectangular $14 \times 11 \times 90$ mm specimens where extracted from center of the component, along the filament to ensure homogeneous composition. These specimens were analyzed with a GrindoSonic MK5 system according to ASTM 215 standard. Fig. 16 presents a correlation of the dynamic E and the density of the material.

As detailed in Craveiro et al. [41], the strength of these mixtures (M0cork and M10cork) linearly decreases with the increase of cork, as well as its density. On the other hand, concrete materials are quasi-brittle materials with nearly linear E. The correlation shown in Fig. 16 is almost linear, emphasizing the expected cork distribution. These results are a preliminary and interesting examination which introduce a future extensive research focused correlating the dynamic modulus of elasticity with the addition of cork.

3.2.2.1. Thermal simulation. The thermal performance of the functionally graded wall block unit was determined using Autodesk Ecotect Analysis software, allowing the calculation of total yearly energy consumption by a building, utilizing a global weather database. Two cities, in two different locations were considered: Lisbon (Portugal) in Southern Europe and State College (Pennsylvania, USA) in North America.

To calculate the thermal performance of the produced graded material, a room with 3 m × 3 m × 3 m was designed, and the material properties of the walls and the roof were assigned. Due to limitations of the Ecotect in representing material gradients, the walls were divided in 8 homogeneous layers. Each layer, with 0.025 m of thickness, had specific associated characteristics, such as specific heat, thermal conductivity, and density, according to the position. Considering an air conditioning system with 95 % efficiency, the monthly heating and cooling loads required to preserve a comfort temperature (18 − 25 °C) over a one-year period in Lisbon and State College were analyzed considering two different material compositions: homogeneous material (M0cork) and functionally graded material (M10cork to M0cork). The functionally graded one was tested in two different ways, first considering a material with 10 % of cork in the outdoor side and gradually changing to 0% of cork in the indoor side, while the second way was the opposite.

Results summarized in Table 2 show that gradient solutions are better energy efficient solutions. It can be also observed that when cork gradation decreases from the outdoor to the indoor of the building, there is a need of fewer energy to keep comfort temperature.

In this work, a functionally graded wall block unit containing up to of 10 % of cork was produced and tested. This graded material solution is 3% lighter than a homogeneous one with no cork.

On the other hand, if 30 % of cork instead of 10 % had been used, a decrease of 17 % in weight and savings of 10.6 % and 13.4 % of energy for State College and Lisbon respectively, would be observed. Additionally, it should be noted that M0cork mixture, specially formulated with basalt sand and different additives, already presents a lower thermal conductivity (0.82 W/[m × K]) compared with the same mixture using river sand instead of basalt sand, even with no cork. If a standard mixture containing river sand as aggregate (thermal conductivity = 1.68 W/[m × K]) had been used, an addition of 118.7 % (Lisbon) and 82.2 % (State College) in energy consumption would be required.

3.3. Discussion

Today, material extrusion is the most widely used technology to produce homogeneous concrete structures by AM [18]. As such, an AM system capable of extruding functionally graded concrete was developed and presented in this paper. This equipment was tested in two different cases, one consisted in producing homogeneous components and the second involved the manufacture of a functionally graded curved block. Homogeneous components were produced using one single pump working at a constant speed, which allowed to reach 23 layers. Producing homogeneous concrete components was a crucial step to fine-tune the printing system before printing a functionally graded one with success.

The geometry of the printed homogeneous curved block was compared with the predicted design and results present a standard deviation of 4.163 mm. However, in some areas, deviations reaching ~12 mm are visible due to the slide of filaments and material deformation after deposition. To avoid this problem, two solutions are being tested and will be reported in future papers. The first solution is to change the direction of the toolpath among consecutive layers, for instance, by making them perpendicular, rather than using a similar toolpath in all the layers. This strategy can also help reduce residual stress. The second solution is to model material deformation to compensate for this effect in the design of the toolpath.

The materialization of a functionally graded block required two pumps constantly changing its working speed to mix concrete with different aggregates in varying proportions. Internal voids indicate insufficient pumping pressure, creating weak areas; however, results show that material composition distribution corresponded to the predicted in the 3 cross-sections. ImageJ counted all visible granules, from very small (difficult to see) to the bigger ones. Other methods, such as tomography should be used to allow a more accurate investigation of the cork distribution. The small twin concrete pumps have been used as proof of concept, and a maximum of 10 % of cork was selected due to its lack of pressure to extrude materials containing more cork. However, an industrial pump (m-tec Duomix 2000) was acquired and is being employed to study the impact of various variables (system, materials, shape design and environmental conditions) in the production of cement-based homogeneous components [45]. To prevent the formation of internal voids, in these tests both the extrusion head and its distance to the printed bead have been modified to press the deposited material down causing it to adhere to the side filament and the filament below (Fig. 17).

The next step is to purchase a second industrial pump to study the same variables mentioned above but for functionally graded materials, using the software and speed control modules already developed for the small pumps. The results presented in this work are promising and indicate the need for further material testing (i.e. viscosity, printing speed, direction of fibers, residual stress), preferably extruded with the industrial pumps. It will also be important to produce multiple samples to verify the consistency of the experimental results.

4. Conclusions

This research work presents a novel AM system to produce single material and multi-material functionally graded concrete structures. Both software and hardware elements of the new 3D printing proposed system were detailed, showing its high versatility in terms of design and making of optimized building parts by manipulating material composition. Different structures were successfully printed. The system offers great potential to create lightweight building parts with improved thermo-mechanical properties. Maximizing cork quantity optimizes the thermal insulation and decreases weight whereas minimizing its amount increases mechanical performance. This system has the

Table 2
Heating and cooling loads needed to maintain the comfort temperature over a one-year period.

Material	Location	Heating/Cooling loads (kWh)		
		Heating	Cooling	Total
M0cork (reference)	Lisbon	1349.857	462.784	1812.641
	State College	4094.903	254.224	4349.127
M10cork	Lisbon	1330.978 (-1.4 %)	446.090 (-3.6 %)	1777.068 (-2%)
(from 10 % cork in the outdoor to 0% cork in the indoor)	State College	4038.030 (-1.4 %)	247.194 (-2.8 %)	4285.224 (-1.5 %)
M10cork	Lisbon	1331.244 (-1.4 %)	465.111 (+0.5 %)	1796.355 (-0.9 %)
(from 0% cork outdoor to 10 % cork in the indoor)	State College	4038.816 (-1.4 %)	257.735 (+1.4 %)	4296.550 (-1.2 %)

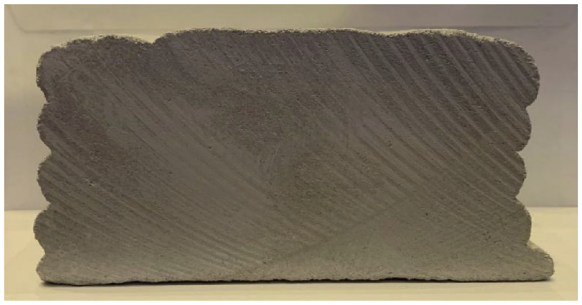

Fig. 17. Cross-section of a part produced with the M-Tec Duomix 2000 pump.

potential to minimize waste (reusing rejected natural materials) and CO_2 emissions by improving material efficiency and sustainability. It was possible to demonstrate the production of a functionally graded concrete, which material composition changes according to a predefined distribution. Future developments will include new material formulations and experimental studies on printed elements, focusing on structural stability and integrity.

Credit author statement

The paper presents a system to produce functionally graded concrete parts by replacing sand with cork as aggregate. Flavio is the PhD student who carried out the research, advised by H. Bartolo in civil engineering, P. Bartolo in mechanical engineering, S. Nazarian in material matters and J. Duarte in design computing aspects, who also supervised the work.

Declaration of Competing Interest

The authors declare that they have no known competing financial interests or personal relationships that could have appeared to influence the work reported in this paper.

Acknowledgments

This research work was supported by grant SFRH/BD/105404/2014 from the Portuguese Foundation for Science and Technology (FCT); by Seed Grant Opportunity on Convergence between Materials and Energy from both the Material Research Institute (MRI) and the Institute for Energy and Environment (PSIEE); and by The Raymond A. Bowers Program for Excellence in Design and Construction of the Built Environment, The Pennsylvania State University.

Appendix A. Supplementary data

Supplementary material related to this article can be found, in the online version, at doi:https://doi.org/10.1016/j.addma.2020.101146.

References

[1] M. Shomberg, How Digitization Is Disrupting Construction: Strategies Forward, Digitalist Magazine, 2016 Available at: https://www.digitalistmag.com/iot/2016/08/25/digitization-disrupting-construction-strategies-forward-04417204 (Accessed: 28 October 2018).
[2] ISO/ASTM 52900, Additive Manufacturing – General Principles – Terminology, International Organization for Standardization, 2015 Available at: https://www.iso.org/obp/ui/#iso:std:iso-astm:52900:ed-1:v1:en (Accessed: 04 January 2019).
[3] S.C. Paul, G.P.A.G. van Zijl, M.J. Tan, I. Gibson, A review of 3D concrete printing systems and materials properties: current status and future research prospects, in: R.I. Campbell, R.I. Campbell (Eds.), Rapid Prototyping Journal, 2018, pp. 784–798.
[4] F. Craveiro, J.P. Duarte, H. Bártolo, P.J. Bártolo, Additive Manufacturing as an enabling technology for digital construction: a perspective on Construction 4.0, Autom. Constr. 103 (2019) 251–267.
[5] P. Wu, J. Wang, X. Wang, A critical review of the use of 3-D printing in the construction industry, Autom. Constr. 68 (2016) 21–31.
[6] Y.W.D. Tay, B. Panda, S.C. Paul, N.A. Noor Mohamed, M.J. Tan, K.F. Leong, 3D printing trends in building and construction industry: a review, Virtual Phys. Prototyp. 12 (3) (2017) 261–276.
[7] Winsun, Winsun – 3D Printing Architecture's Future, Available at: http://www.winsun3d.com/En/About/ (Accessed: 20 July 2018) (2014).
[8] Apis Cor, Apis Cor – We Print Buildings, Available at: http://apis-cor.com/en/3d-printer (Accessed: 20 July 2018) (2016).
[9] T.A.M. Salet, Z.Y. Ahmed, F.P. Bos, H.L.M. Laagland, Design of a 3D printed concrete bridge by testing, Virtual Phys. Prototyp. 13 (3) (2018) 222–236.
[10] R.A. Buswell, W.R. Leal de Silva, S.Z. Jones, J. Dirrenberger, 3D printing using concrete extrusion: a roadmap for research, Cem. Concr. Res. 112 (2018) 37–49.
[11] C. Gosselin, R. Duballet, P. Roux, N. Gaudillière, J. Dirrenberger, P. Morel, Large-scale 3D printing of ultra-high performance concrete – a new processing route for architects and builders, Mater. Des. 100 (2016) 102–109.
[12] N. Oxman, Variable property rapid prototyping, Virtual Phys. Prototyp. 6 (1) (2011) 3–31.
[13] S. Sing, S. Ramakrishna, R. Singh, Material issues in additive manufacturing: a review, J. Manuf. Process. 25 (2017) 185–200.
[14] C.M.R. Dias, H. Savastano Jr, V.M. John, Exploring the potential of functionally graded materials concept for the development of fiber cement, Constr. Build. Mater. 24 (2) (2010) 140–146.
[15] K.M. Gupta, Engineering Materials: Research, Applications and Advances, CRC Press, Boca Raton, Fla, 2014.
[16] H. Van Damme, Concrete material science: past, present, and future innovations, Cem. Concr. Res. 112 (2018) 5–24.
[17] M. Herrmann, W. Sobek, Functionally graded concrete: numerical design methods and experimental tests of mass-optimized structural components, Struct. Concr. 18 (1) (2017) 54–66.
[18] D. Delgado Camacho, P. Clayton, W.J. O'Brien, C. Seepersad, M. Juenger, R. Ferron, S. Salamone, Applications of additive manufacturing in the construction industry – a forward-looking review, Autom. Constr. 89 (2018) 110–119.
[19] A.K. Ray, S. Mondal, S.K. Das, P. Ramachandrarao, Bamboo—a functionally graded composite-correlation between microstructure and mechanical strength, J. Mater. Sci. 40 (19) (2005) 5249–5253.
[20] N. Oxman, Programming matter, Archit. Des. 82 (2) (2012) 88–95.
[21] F. Craveiro, H. Almeida, L. Durão, H. Bártolo, P.J. Bártolo, Rapid construction with functionally graded designs, Green Design, Materials and Manufacturing Processes, Taylor & Francis, London, 2013.
[22] F. Craveiro, H. Bártolo, J.P. Duarte, P.J. Bártolo, A strategy to locally optimize the material composition of am construction elements, Proceedings of the 2nd International Conference on Progress in Additive Manufacturing, Singapore: Research Publishing, 2016, pp. 188–193.
[23] S. Keating, N. Oxman, Compound fabrication: a multi-functional robotic platform for digital design and fabrication, Robot. Comput. Manuf. 29 (6) (2013) 439–448.
[24] R.W.S. Chee, W.L. Tan, W.H.G. Goh, F. Amtsberg, S. Dritsas, Locally differentiated concrete by digitally controlled injection, Learning, Adapting and Prototyping - Proceedings of the 23rd CAADRIA Conference, Beijing, China: Tsinghua University, 2018, pp. 195–204. Available at: http://papers.cumincad.org/data/works/att/caadria2018_156.pdf (Accessed: 07 August 2018).
[25] R.M. Mahamood, E. Akinlabi, M. Shukla, S. Pityana, Functionally graded material: an overview, Proceedings of the World Congress on Engineering 2012. World Congress on Engineering, Newswood Limited, London, 2012, pp. 2–6.
[26] F. Craveiro, H. Almeida, H. Bártolo, P.J. Bártolo, J.P. Duarte, Topology and material optimization of architectural components, in: F. Moreira da Silva, H. Bártolo, P.J. Bártolo, R. Almendra, F. Roseta, H. Almeida, A.C. Lemos (Eds.), Challenges for Technology Innovation: An Agenda for the Future, CRC Press, London, 2017, pp. 71–76.
[27] F. Bos, R. Wolfs, Z. Ahmed, T. Salet, Additive manufacturing of concrete in construction: potentials and challenges of 3D concrete printing, Virtual Phys. Prototyp. 11 (3) (2016) 209–225.
[28] European Commission, Directive 2008/98/EC of the European Parliament and of the Council of 19 November 2008 on Waste and Repealing Certain Directives, Available at: http://data.europa.eu/eli/dir/2008/98/oj (Accessed: 10 November 2018) (2008).
[29] J.M. Kanema, J. Eid, S. Taibi, Shrinkage of earth concrete amended with recycled aggregates and superplasticizer: impact on mechanical properties and cracks, Mater. Des. 109 (2016) 378–389.
[30] T. Kim, S. Tae, C. Chae, Analysis of environmental impact for concrete using LCA by varying the recycling components, the compressive strength and the admixture material mixing, Sustainability 8 (4) (2016) 389.
[31] F.L. Gayarre, J.S. González, M.A.S. López, C.L.-C. Pérez, P.J.F. Arias, Mechanical properties of prestressed joists made using recycled ceramic aggregates, Constr. Build. Mater. 194 (2019) 132–142.
[32] S. Ramdani, A. Guettala, M. Benmalek, J.B. Aguiar, Physical and mechanical performance of concrete made with waste rubber aggregate, glass powder and silica sand powder, J. Build. Eng. 21 (2019) 302–311.
[33] A. Costa, E. Júlio, J. Lourenço, A new mixture design method for structural lightweight aggregate concrete, 8th Fib PhD Symposium in Kgs. 8th Fib PhD Symposium in Kgs, (2010) Lyngby, Denmark.
[34] A. Brás, M. Leal, P. Faria, Cement-cork mortars for thermal bridges correction. Comparison with cement-EPS mortars performance, Constr. Build. Mater. 49 (2013) 315–327.
[35] A.M. Matos, S. Nunes, J. Sousa-Coutinho, Cork waste in cement based materials, Mater. Des. 85 (2015) 230–239.
[36] F. Craveiro, H. Bártolo, P.J. Bártolo, Functionally graded structures through building manufacturing, Adv. Mat. Res. (2013) 775–778.
[37] F. Craveiro, H.M. Bartolo, A. Gale, J.P. Duarte, P.J. Bartolo, A design tool for

resource-efficient fabrication of 3d-graded structural building components using additive manufacturing, Autom. Constr. 82 (2017) 75–83.
[38] F. Craveiro, J.P. Matos, H. Bártolo, P.J. Bártolo, et al., Automation for building manufacturing, in: P.J. Bártolo (Ed.), Innovative Developments in Virtual and Physical Prototyping, CRC Press, London, 2011.
[39] F. Craveiro, H. Almeida, H.M. Bártolo, J.P. Duarte, P.J. Bártolo, Designing cork-based functionally graded concrete walls, in: F. Moreira da Silva, H. Bártolo, P.J. Bártolo, R. Almendra, F. Roseta, H. Almeida, A.C. Lemos (Eds.), Challenges for Technology Innovation: An Agenda for the Future, CRC Press, London, 2017, pp. 431–434.
[40] F. Craveiro, H. Bártolo, P.J. Bártolo, S. Nazarian, J.P. Duarte, Additive manufacturing of functionally graded building parts: towards seamless architecture, 4th Biennial Residential Building Design & Construction Conference Proceedings, State College: Pennsylvania Housing Research Center, 2018, pp. 529–540. Available at: https://www.phrc.psu.edu/assets/docs/Publications/2018RBDCCPapers/2018-RBDCC-Whole-Proceedings.pdf.
[41] F. Craveiro, H. Bártolo, P.J. Bártolo, J.P. Duarte, Characterization of concrete/cork Materials for Functionally Graded Additive Manufacturing, [Manuscript submitted for publication] (2019).
[42] M. Hojati, S. Nazarian, J.P. Duarte, A. Radlińska, N. Ashrafi, F. Craveiro, S. Bilén, 3D printing of concrete: a continuous exploration of mix design and printing process, Proceedings of the 42nd IAHS World Congress on The Housing for the Dignity of Mankind, Naples, Italy, 2018.
[43] F. Craveiro, H. Bartolo, J.P. Duarte, P.J. Bartolo, et al., A multi-material extrusion nozzle for functionally graded additive manufacturing, in: P.J. Bártolo (Ed.), Industry 4.0 – Shaping the Future of the Digital World, Taylor & Francis, London, 2019.
[44] NIH, ImageJ Features, Available at: https://imagej.nih.gov/ij/features.html (Accessed: 20 December 2018) (2018).
[45] N. Ashrafi, J.P. Duarte, S. Nazarian, N.A. Meisel, Evaluating the relationship between deposition and layer quality in large-scale additive manufacturing of concrete, Virtual Phys. Prototyp. 14 (2) (2019) 135–140.